DCATT Dispersed Fringe Sensor: Modeling and Experimenting with the Transmissive Phase Plates

Fang Shi[a], Dave Redding[a], Chuck Bowers[b], Andrew Lowman[a], Scott Basinger[a], Todd Norton[b], Peter Petrone[b], Pam Davila[b], Mark Wilson[b], and Ray Boucarut[b]

[a]Jet Propulsion Laboratory, California Institute of Technology, Pasadena, CA 91109
[b]Goddard Space Flight Center, NASA, Greenbelt, MD 20771

ABSTRACT

Control algorithms developed for coarse phasing the segmented mirrors of the Next Generation Space Telescope (NGST) are being tested in realistic modeling and on the NGST wavefront control testbed, also known as DCATT. A dispersed fringe sensor (DFS) is used to detect piston errors between mirror segments during the initial coarse phasing. Both experiments and modeling have shown that the DFS provides an accurate measure of piston errors over a range from just under a millimeter to well under a micron.

Keywords: Space telescope, wavefront detection, dispersed fringe sensor

1. INTRODUCTION

The proposed Next Generation Space Telescope (NGST) design uses deployed, segmented primary mirror optics and a deployed secondary mirror. After deployment on orbit, the segments will need to be aligned and phased. The initial wavefront errors may be very large (~ cm) and the final phased wavefront should provide diffraction limited imagery at 2 μm wavelength. The whole process is split into distinct stages including: (1) initial target capture, segment mirror coarse alignment and focusing, which bring the wavefront errors down from centimeters to sub-millimeter; (2) coarse phasing using dispersed fringe sensor (DFS) and white light interferometery (WLI), which bring the wavefront errors down from sub-millimeter to sub-micron; and (3) fine phasing using the phase retrieval which bring the wavefront errors further down to a few nanometers range. The entire process uses images from the science camera instead of a dedicated wavefront sensor system [1, 2]. Realistic optical model and control algorithms have been developed and a control software package has been integrated to DCATT testbed hardware [3].

The dispersed fringe sensor (DFS) measures piston errors between the segmented mirrors in the process of the coarse phasing. DFS uses a transmissive grism in the filter wheel of the imaging camera as the dispersing element. It spreads the light according to its wavelength, forming a spectrum on the camera. Coherent addition of the wavefront error due to the relative piston of the segment mirrors will result in the intensity modulation on the spectrum. The field intensity at any points E(x) along the dispersion is the sum of the fields from the de-phased segments:

$$E(x) = E_1 e^{i(2\pi/\lambda(x)L)} + E_2 e^{i(2\pi/\lambda(x)(L+\delta L))}$$

where E_1 and E_2 are the amplitude the two segments, L is the diffraction length and δL is the phase jump due to the piston between the segments. Along the dispersed spectrum the wavefronts may add constructively or destructively, depending on the local wavelength and the global piston error. Periodic dark bands are formed within the point-spread-function (PSF) when λ is such that the destruction condition $(2\pi/\lambda)\delta L = \pi/2$ is met.

2. DCATT DFS MODELING AND CONTROL ALGORITHM

Developmental Comparative Active Telescope Testbed (DCATT) was designed and developed to test wavefront control technology. Its primary mirror has seven hexagonal segment mirrors with total diameter of 1 meter. Reflecting by a flat mirror in front of the telescope, light from the source stimulus model will double pass through the telescope optics [4]. A double-pass DCATT optical model with transmissive grism as the dispersing element has been built using MACOS, an optical modeling tool. In this realistic model optical elements as well as their kinematic controls are built to reflect the real

hardware of the testbed. The model is used to simulate the DFS fringes including effects of segment alignment and figure errors. A fringe analysis algorithm is used to detect the piston error from the DFS fringe signals and then drive the actuators of the segment mirror to correct these piston errors. In the DFS fringe analysis the optical path difference (OPD) due to the piston error is derived from the DFS signal using a least-squares fit to a standard fringe formula. The DFS control software is developed as a part of the wavefront control software for DCATT. It has a GUI which provides control input and status display and it works both on the DCATT model and hardware. The functions include taking the DFS fringe image, calibrating the DFS, processing the DFS image and extracting the DFS signal, analyzing DFS signal and controlling the DCATT segment mirrors to correct the piston error. Fig. 1 shows the DFS fringe image and signal generated by the model. The modeling has shown:

(1) The DFS modulation period depends on the relative piston error with more fringes at larger piston error.
(2) The visibility of the DFS fringe depends on the orientation of the direction of the dispersion relative to the baseline between segment pairs, with the highest visibility occurring when they are orthogonal.
(3) The sign of the piston can be determined by the angle the fringe makes across the spectrum.
(4) The DFS sensitivity range depends on the total bandwidth of the spectrum as well as the spatial sampling rate of the camera. DFS with higher spectral bandwidth can detect smaller piston error and the largest piston error DFS can detect is limited by the capability of the camera to resolve the DFS fringe modulation. For the current DCATT setup, the DFS can detect the piston error from sub-millimeter to sub-micron.
(5) The accuracy of the OPD derived from DFS fringe analysis also depends on the accuracy of the DFS wavelength calibration.
(6) The DCATT DFS can tolerate segment tilt mis-alignment (mis-centering) up to 0.1 arc-second.
(7) The DCATT DFS can tolerate a few waves of mirror surface aberrations without losing its sensitivity although not all the aberrations have the same effect on the DFS.

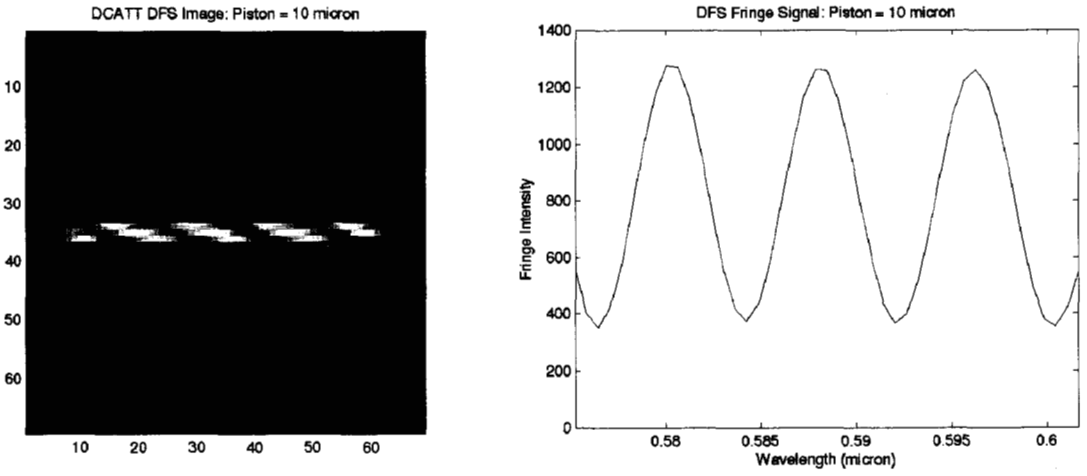

Figure 1. Typical DFS model fringe image and signal.

3. DFS EXPERIMENT USING TRANSMISSIVE PHASE PLATES

First experiments using the dispersed fringe sensor have been done on DCATT. This experiment was a preliminary test for DFS because the segmented DCATT telescope had yet to be manufactured and integrated. To generate a piston error into the wavefront fused silica plates with half of the area being etched out were used. The etched phase plates with physical step sizes from 0.5 μm to 10 μm were used in the stimulus module of the DCATT, creating the wavefront pistons from 0.5 μm to 10 μm. DFS wavelength calibration was done using five narrow band filters (bandwidth = 3 nm) with wavelength centered from 515 nm to 795 nm. A reference DFS image which contains the intrinsic spectrum of the white light source (a Xe arc lamp) was also taken as part of the calibration.

DFS image processing includes removing the dark frame, removing the spectral influence of the source and CCD response using the reference DFS image and further removing the detector noise by filtering. The DFS signals were then extracted from the processed DFS image and the wavefront piston error was derived using the DFS fringe analysis software. The

bandwidth of the DFS spectra was 280 nm (from 515 nm to 795 nm). Fig. 2 and Fig. 3 show some of the DFS images, DFS signals and their solution fits.

Table 1. lists experimental results for piston error detection by the DFS. The table has converted the wavefront piston errors into the physical step size of the phase plate. The physical step sizes of the phase plates have been measured with a Wyko TOPO. The experiment results show that DFS can accurately measure the piston errors caused by the phase plates except for the smallest step size (0.5 μm). For the experiment setup the OPD from the 0.5 μm phase plate was too small to have a complete modulation cycle.

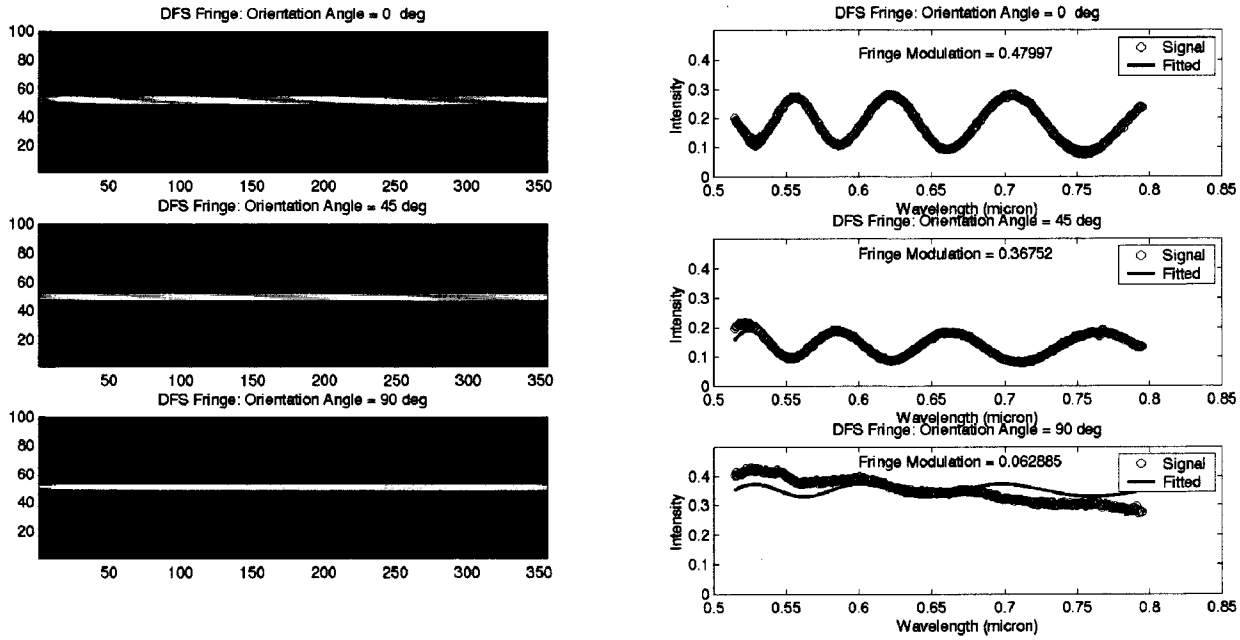

Figure 2. DFS images and signals for the 5 micron phase plate.

Table 1. Phase plate step sizes and the DFS measurements.

Phase Plate Step Size (μm)	0.525	2.08	2.54	5.14	10.0
DFS Measurement (μm)	0.034±0.05	1.98±0.085	2.47±0.195	5.26±0.265	10.17±0.115
Number of Measurements	3	6	6	5	3

Figure 2 shows DFS images and their signals for the 5 μm phase plate. The three DFS images were taken with the phase plate dividing line at parallel (top), 45 degree (middle) and orthogonal position (bottom) relative to the DFS dispersion direction. The figure shows that the visibility (modulation) of the DFS fringe depends on the orientation of the dispersion relative to the base line of the segment pairs. This confirms the prediction of the DFS models.

Figure 3 shows the DFS images and their signals for the 10 μm phase plate. The images and the plots show the relation between the sign of OPD and the orientation of the glancing dark bands. To generate the OPD sign flip the phase plate rotated 180 degree between these two images. On the DFS signal plots, three DFS signals are extracted from the image, the main DFS signal and the signals a row up and a row down from the main signal. In the DFS fringe analysis software the relative "peak" or "valley" positions among the three signals are used to determine "glancing" orientation of the dark bands hence the sign of the OPD.

4. CONCLUSION AND DISCUSSION

The DFS experiments using transmissive phase plates have provided us with critical data in our development of the wavefront control technology for NGST. The experiment has confirmed many DFS modeling results. The experiment has also tested the DFS imaging process and the fringe analysis algorithm in the DCATT DFS control software with the real image data with non-uniform spectral influence. However, due to delays for the DCATT telescope, the closed loop operation has yet to be tested. Analysis of the experiment results has shown that the DFS can detect piston errors from sub-millimeter to sub-micron range, confirming its utility in the NGST coarse phasing process. The DFS algorithm is proved to be robust, repeatable and accurate, and the detection also provide the OPD sign information which enables the DFS to direct control the segment mirror during the coarse phasing process. The DFS measurement of the step sizes has agreed with the direct measurements by a white light interference microscope within 5%. Analysis has indicated the wavefront measurement errors shown in Table 1 are contributed by the DFS wavefront calibration errors, small transverse sampling by the CCD camera and DFS images taken with non-orthogonal orientation of dispersion relative to the segment base line.

Further experimentation with the DFS is needed to validate the wavefront control part of the software. A new grism with higher dispersion power will replace the current one to provide better pixel sampling for the camera. This will increase the DFS detection range. A new telescope simulator with three small segmented spherical mirrors has now been developed and more results will be coming soon from this unique testbed.

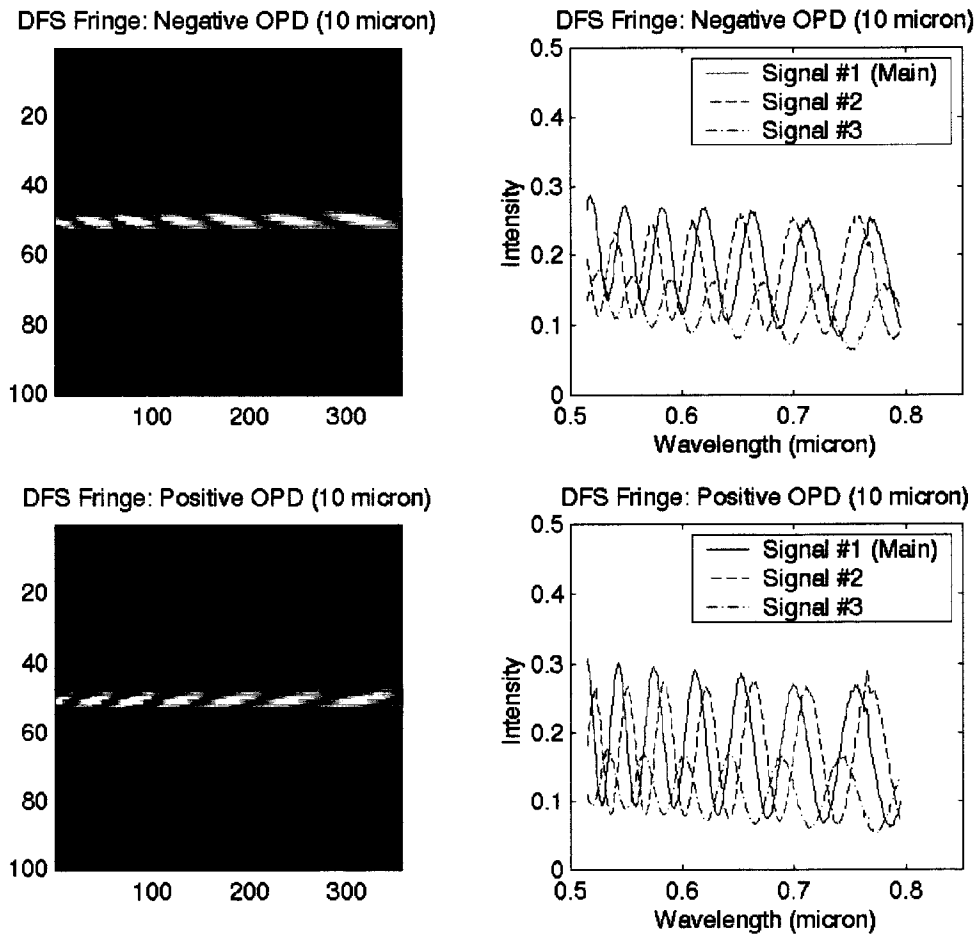

Figure 3. DFS images and signals for 10 micron phase plate.

5. ACKNOWLEDGEMENT

The authors are indebted to Michael Shao for bringing the DFS technique to our attention. This work was performed at the Jet Propulsion Laboratory, California Institute of Technology, under contract with NASA.

6. REFERENCES

1. D. Redding, S. Basinger, A. Lowman, F. Shi, P. Bely, R. Burg, G. Mosier, "Wavefront Sensing and Control for a Next Generation Space Telescope," SPIE 3356-47, 1998, http://ngst.gsfc.nasa.gov/public/unconfigured/doc_440_1/ngstWFC.pdf.
2. D. Redding, S. Basinger, A. Lowman, F. Shi, C. Bowers, L. Burns, P. Davila, B. Dean, M. Fitzmaurice, J. Hagopian, C. Leboeuf, G. Mosier, T. Norton, B. Perkins, P. Petrone, L. Wheeler, M. Wilson, "Performance of the NGST Wavefront Control System as Tested on DCATT," NGST Science and Technology Symposium, Hyannis MA, Sept. 1999.
3. S. Basinger, D. Redding, F. Shi, B. Smith, L. Burns, B. Perkins, G. Mosier, L. Wheeler, J. Deering, A. Lowman, "Controlling the DCATT/NEXCAT Hardware," NGST Science and Technology Symposium, Hyannis MA, Sept. 1999.
4. C. Leboeuf, P. Davila, D. Redding, A. Morell, A. Lowman, M. Wilson, E. Young, L. Pacini, D. Coulter, "Developmental cryogenic active telescope testbed, a wavefront sensing and control testbed for the next generation space telescope," http://dcatt.gsfc.nasa.gov/documents/papers/3356-72.pdf.